Combined single-crystal X-ray and neutron powder diffraction structure analysis exemplified through full structure determinations of framework and layer beryllate minerals

JENNIFER A. ARMSTRONG,[1] HENRIK FRIIS,[2] ALEXANDRA LIEB,[1,*] ADRIAN A. FINCH,[2] AND MARK T. WELLER[1,†]

[1]School of Chemistry, University of Southampton, Highfield, Southampton, Hampshire SO17 1BJ, U.K.
[2]School of Geography and Geosciences, Irvine Building, University of St. Andrews, North Street, St. Andrews, Fife KY16 9AL, U.K.

ABSTRACT

Structural analysis, using neutron powder diffraction (NPD) data on small quantities (<300 mg) and in combination with single-crystal X-ray diffraction (SXD) data, has been employed to determine accurately the position of hydrogen and other light atoms in three rare beryllate minerals, namely bavenite, leifite/IMA 2007-017, and nabesite. For bavenite, leifite/IMA 2007-017, and nabesite, significant differences in the distribution of H, as compared to the literature using SXD analysis alone, have been found. The benefits of NPD data, even with small quantities of H-containing materials, and, more generally, in applying a combined SXD-NPD method to structure analysis of minerals are discussed, with reference to the quality of the crystallographic information obtained.

Keywords: Hydrogen, beryllium, minerals, powder neutron diffraction

INTRODUCTION

Information on crystal structure of minerals, including the localization of light atoms such as H and Be, is of considerable importance because it allows a better understanding of the mineral behavior under natural conditions. This includes information on a mineral's paragenesis, phase stability, compressibility/water content, and thermal expansion. In mineralogy, most characterization methods are based on X-ray diffraction for structures and the detection of element-characteristic X-rays for chemical analyses. Unfortunately, the weak scattering power of light elements combined with the low energy of their characteristic X-rays make it nontrivial to study minerals that contain such elements. This is a particular problem for Be minerals that also contain heavy elements, which dominate the X-ray diffraction and also produce strong X-ray absorption, making some aspects of structure and compositional analysis problematic.

Known three-dimensional tectosilicate framework structures are formed mainly from AlO_4 and SiO_4 tetrahedra and include about 80 different natural zeolites structures (Baerlocher et al. 2007). However, many natural minerals with structures formed from linked tetrahedral units are not simple silicates or aluminosilicates, but also incorporate other framework forming species such as the beryllate tetrahedron, BeO_4, or oxo/hydroxo/fluoroberyllate $Be(O,OH,F)_4$, sometimes written $Be\varphi_4$, within their structures. The beryllate unit, while of similar dimensions to the silicate tetrahedron [the distances Be-O in BeO_4 and Si-O in SiO_4 are both typically ~1.61(4) Å (Hawthorne and Huminicki 2002)], often produces quite different structure types due to the lower cation charge, Be^{2+} vs. Si^{4+}. Thus, a bridging or terminal O forming part of a $Be\varphi_4$ tetrahedron is under-bonded compared to the equivalent $Si\varphi_4$ unit leading to the prevalence of Be-OH and Be-F in beryllate minerals (Hawthorne and Huminicki 2002). The role of the H-containing species such as H_2O and OH groups is also important in determining the structure and distribution of non-framework species in many silicate and beryllate minerals.

Structural information extracted using conventional X-ray techniques has limitations in being insensitive to light atoms, and sites for species such as H and Be are often only proposed on the basis of bond length arguments and chemical composition. In structures where H-containing species show atypical bond lengths, unusual interactions with neighboring species (e.g., strong hydrogen bonds), or several structurally reasonable positions exist, additional data are needed to define the true light atom positions. Where possible, single-crystal neutron diffraction (SND) data can be analyzed, but the need for large high-quality single crystals often limits the scope of this technique in its application to minerals. Neutron powder diffraction (NPD) data are also sensitive to light atoms, but potential problems include the need for reasonably large sample sizes, typically a few grams, on low-flux neutron diffractometers. For H-containing minerals, the large incoherent scattering from H can severely degrade data quality by producing very high backgrounds and, therefore, potentially low signal to noise ratios for the diffraction peaks. Deuteration, the normal route used to avoid incoherent scattering, is generally impossible for mineral samples where the H is tightly bound and not amenable to H/D exchange. With some modern, high-flux NPD instrumentation, very small samples can be studied, for example the recent study of 4.5 mg of the mineral tooeleite (P.F. Henry, personal communication) on the D20 instrument at the Institut Laue-Langevin (ILL), Grenoble (Hansen et al. 2008). High-flux instrumentation also has the

* Current address: Institut für Anorganische Chemie, Christian-Albrechts-University of Kiel, Max-Eyth-Strasse 2, D-24118 Kiel, Germany.
† E-mail: M.T.Weller@soton.ac.uk

advantage of markedly improving the signal to noise ratio as a result of rapid time-averaging of the incoherent scattering; this allows H-containing materials to be studied directly, for example the recent study of goosecreekite (Henry et al. 2008). Where only a small quantity of a sample is available, NPD data can successfully be combined with structure data obtained using X-ray methods (Weller et al. 2007). This technique is widely applicable and allows the accurate determination of positional and atomic displacement parameters for all atom types including H when only small samples are available and the NPD data may not be of the highest quality. An additional advantage of studying H-containing minerals using neutron diffraction is that the coherent scattering length of H is negative at –3.34 fm (compared with deuterium's positive value +6.67 fm); as a result difference Fourier maps calculated using observed and calculated neutron diffraction structure factors readily locate H as "negative" peaks.

In this paper, we evaluate the method's applicability to complex minerals and report the structures of three rare beryllate minerals, namely bavenite, leifite/IMA 2007-017, and nabesite. Because of mineral rarity, NPD data have been collected from only small samples (<300 mg) and been analyzed to extract structural information in combination with single-crystal X-ray diffraction (SXD) data. These minerals were chosen as several structural features were poorly defined in previous single-crystal X-ray diffraction studies, i.e., in some minerals the H position(s) is either not given, assumed, or imprecise. Additionally, the NPD-SXD combined data analysis technique also allows better determination of the distribution of Si, Al, and Be in the framework in some cases giving overall improved structure descriptions.

DESCRIPTION, MINERALOGY, AND STRUCTURE OF SAMPLES

Bavenite was first described from Baveno, Italy, by Artini (1901). He failed to recognize the presence of Be in this mineral, which was first found by Schaller and Fairchild (1932). Petersen et al. (1995) first recorded bavenite in the Ilímaussaq alkaline complex, South Greenland, and determined the unit cell from powder X-ray diffraction (PXD) data. The Ilímaussaq bavenite is orthorhombic, $Cmcm$, $a = 23.212(3)$ Å, $b = 4.993(1)$ Å, and $c = 19.480(3)$ Å, which corresponds reasonably well with specimens obtained from Baveno, Italy. The formula for bavenite is $Ca_4[Be_{(2+x)}Al_{(2-x)}Si_9O_{(26-x)}(OH)_{(2+x)}]$ where $0 \leq x \leq 1$ (Beus 1960). The determined chemical composition of Ilímaussaq bavenite corresponds to the empirical formula $Ca_4[Be_{3.5}Al_{1.0}Si_9O_{26.1}(OH)_{1.9}]$, and the infrared spectrum shows sharp peaks from well-defined OH-groups (Petersen et al. 1995). The crystal structure of bavenite was initially solved by Cannillo et al. (1966) from a three-dimensional Patterson synthesis. Six tetrahedral sites have been proposed of which Si is ordered into four, Al into one, and Be into one of those six sites. The tetrahedra create two different 6-membered rings that, when connected into a 3-dimensional framework, create large channels that accommodate the Ca^{2+} ions. Cannillo et al. (1966) proposed the position for an H atom connected to the O atom (designated O8 in that work) on the basis of electrostatic valence calculations and the presence of a weak maximum in a difference Fourier map. Our

sample is from the find described by Petersen et al. (1995) and was donated by the Geological Museum in Copenhagen.

Leifite was first described from the Narssârssuk Pegmatite, Gardar Province, South Greenland, by Bøggild (1915), although he failed to identify Be in the samples. Micheelsen and Petersen (1970) re-analyzed the type material and found it to contain Be. The crystal structure was solved by Coda et al. (1974) in space group $P3m1$ and consists of four different tetrahedral sites. Aluminum and Si are disordered over one site (T1), T2 and T3 are filled with Si, and T4 is a BeO_3F tetrahedron. The structure consists of a six-membered ring of T1 tetrahedra and a seven-membered ring of all tetrahedra, resulting in the formation of channels parallel to the c axis. Channels formed by the six-membered rings host a site that contains mixed cationic species, Cs, K, Na, etc., whereas only sodium ions are accommodated in the sites involving coordination from O atoms of the seven-membered ring. The structure was confirmed by Sokolova et al. (2002) who also proposed the general formula $ANa_6[Be_2Al_3Si_{15}O_{39}F_2]$, $A =$ Na, Cs (for leifite and telyushenkoite, respectively). Published compositions of leifite show great variations in especially H_2O or OH and K content, and a K end-member has been recently approved as a new species from Vesle Arøya, Langesundsfjord, Norway, as IMA 2007-017 (Larsen et al. in prep). In this new species, K dominates the A site of the general formula proposed by Sokolova et al. (2002); for a recent detailed description of the relations between the leifite group members, see Raade (2008). The samples used in this study, termed leifite/IMA 2007-017, formed radiating aggregates on fracture surfaces in a quartzite surrounding parts of the Narssârssuk pegmatite, i.e., the material is not from the actual type locality. The mineral assemblage is very simple and only elpidite and minor feldspar, graphite, and aegirine have been identified.

Nabesite was first found in 1999 and described by Petersen et al. (2002) from one locality on Kvanefjeld, Ilímaussaq alkaline complex, South Greenland, which is still the only known occurrence for this mineral. The ideal formula is $Na_2BeSi_4O_{10} \cdot 4H_2O$ and the structure consists of corner-sharing tetrahedra. Silicon is ordered in four of the five tetrahedral sites, forming sheets of four- and eight-membered rings. The fifth tetrahedron is a BeO_4 tetrahedron, which connects the sheets into a framework where large cations (Na) and H_2O molecules occupy the interstitial space (Petersen et al. 2002). This mineral is found as a late-stage hydrothermal mineral on albite associated with other zeolitic and Be-minerals including lovdarite, chkalovite, tugtupite, analcime, gmelinite, and gonnardite.

EXPERIMENTAL METHODS

All diffraction data were collected on samples cooled to 120 K. The SXD data, cell dimensions, and intensity data were collected on a Bruker-Nonius KappaCCD equipped with a rotating anode (Mo$K\alpha$) and confocal mirrors. For each sample, a small crystal (about $50 \times 50 \times 100$ μm) was selected from hand specimens. The structures were solved using direct methods and refined using full-matrix least-squares via SHELX97 (Sheldrick 2008) to check the quality of the data before using the hkl-files for the joint refinements with the neutron data.

NPD data were collected on hand picked, thoroughly ground material resulting in typical 200–300 mg samples. However, it was only possible to collect 90 mg material of bavenite. The samples were placed in a standard 4 mm cylindrical vanadium sample holder for 1–8 h using the D20 instrument at ILL, Grenoble, France (Hansen et al. 2008). The instrument was set up in its high takeoff angle

setting using a neutron wavelength of 1.87 Å, Ge(115), and fitted with a standard Orange cryostat. Joint NPD-SXD structure refinements were performed using the GSAS suite of programs (Larson and Von Dreele 2004) and the EXPGUI interface (Toby 2001). Alternative Rietveld refinement programs that can be used for such combined data set analysis include JANA2006 (Petricek et al. 2006) and FULL-PROF (Rodríguez-Carvajal 2001). Rietveld refinement was undertaken using the standard methodology using background function 2 (cosine Fourier series) and profile function 2 including all profile parameters (lattice parameters, peak half-width descriptions, zero point, etc.) and atomic positional parameters.

Where joint refinements were undertaken within GSAS the NPD and SXD data sets were given equal weighting for all the reported refinements. It is possible to vary this weighting and the effect of this was investigated up to a ratio of 1:5 in favor of NPD, but with only very minor effects on the extracted atomic parameters. The greater number of independent observations in the SXD data automatically tensions the refinement of the heavier atom positions against these data, while the much greater sensitivity of the NPD data to the H atoms effectively leads to the refinement of these atom positions most strongly against these data. Note that where refinements from SXD data alone are reported, the cell dimensions are those extracted during the data reduction process; where joint SXD-NPD refinements have been undertaken, the cell dimensions reported are those obtained by profile fitting of the NPD data. The GSAS R-factors reported in this work are those described by Larson and Von Dreele (2004) though it is worth commenting on the usefulness of these values with respect to H-containing minerals and the high backgrounds that can be produced in the NPD data. R_p and R_{wp} are the most often quoted for powder diffraction data refinements and measure the difference between the (weighted, for R_{wp}) observed and calculated intensity, y_i, at each point, i, in the profile.

$$R_p = \frac{\sum |y_i(\text{obs}) - y_i(\text{calc})|}{\sum y_i(\text{obs})}.$$

Where a background and therefore the total counts in the diffraction pattern are high, this can lead to unusually low R_p and R_{wp} values, due to the large value of $y_i(\text{obs})$ In these cases, a better measure of the quality of the fit is the R_{F2} value, which is effectively calculated after background subtraction, and values for this fit parameter are given in this paper.

In every case, the most recent structure model from the literature has been used as a starting point for the refinements. The CIFs of the refinements presented in this paper can be found in the electronic supplementary material[1]. The major element composition of selected samples were analyzed on either the Cameca SX50 at the Natural History Museum, London, or on the JEOL JCXA733 electron microprobe at the School of Geography and Geosciences, University of St. Andrews, both operated in wavelength-dispersion mode with an acceleration voltage of 15 kV, and a beam current of 10–20 nA. The beam was defocused and the current was low to minimize Na migration. The following natural and synthetic standards were used: wollastonite (Ca, Si), jadeite or albite (Na), corundum (Al), periclase (Mg), smithsonite or pure metal (Zn), rutile (Ti), orthoclase or KBr (K), LiF (F), CsCl (Cs), and pure metals (Mn, Fe). Intensity data were corrected for inter-element overlaps, and for matrix effects using a Cameca version of the PAP PhiRhoZ program (Pouchou and Pichoir 1984). Beryllium contents were estimated from expected stoichiometry.

RESULTS AND DISCUSSION

The samples were investigated using qualitative EDS, and, because the nabesite sample showed no difference from the composition presented in the literature and in accordance with the aim of this paper, no quantitative analysis was performed on this sample. However, preliminary structure refinements of bavenite and leifite/IMA 2007-017 suggested complicated substitution mechanisms and to achieve better refinement constraints, quantitative analyses were performed for these two samples. The chemical composition used for the structure refinement of

nabesite is presented in Table 1.

The chemical composition of bavenite is presented and compared with the data from Petersen et al. (1995) in Table 2. Our data are in good agreement with previously published data, although our specimen has less Be and Ca compared to Petersen et al. (1995). The empirical formula for our sample is $(Ca_{3.85}Na_{0.05}Zn_{0.02})_{\Sigma 3.92}[Be_{3.04}Al_{0.96}Si_9O_{24.86}(OH)_{3.04}]$, which is close to the ideal formula $Ca_4[Be_3AlSi_9O_{25}(OH)_3]$, and the end-member of the solid solution $Ca_4[Be_{(2+x)}Al_{(2-x)}Si_9O_{(26-x)}(OH)_{(2+x)}]$ with $x = 1$. A joint structure refinement using single-crystal X-ray and NPD data was performed. Table 3 summarizes the unit-cell parameters and other structure refinement data for all the samples studied. During the structure refinement of bavenite, we carefully focused on the framework composition, the distribution of Si, Al, and Be and on potential sites for the protons necessary to balance the framework charge; the quantitative analysis results were not used as hard constraints during the refinement, although refined T-site occupancies were checked against these values. The presence of some Be on the T3 site (nomenclature taken from Cannillo et al. 1966) was evident. Initially, this site was modeled as a mixed Be/Al site, and due to the large differences in the scattering powers for both X-rays and neutrons for these elements, the occupancy factors could be freely refined to 0.546(5) for Al_Si2 and 0.454(5) for Be_Si2 (Table 4a; within the atom names x_y the y indicates the atom site names according to Cannillo et al. 1966). However, as the scattering powers of Si and Al are similar in both X-ray and neutron diffraction, we could not distinguish this model from one in which some Si replaces Al on this site. The slight but significant increase of three of the four T3-O bond lengths (Table 5) compared to the structure model presented by Cannillo et al. (1966) substantiates this model with some Al^{3+} present on the T3 site. To achieve a charge-balanced formula that fits the EPMA measurements, the former Al1 site (T4) was then refined as a mixed Si/Al site, which fits very well to the occurrence of shorter T4-O bonds (average 1.675 Å, typical of a mixed Si/Al site) in our structure model (Table 5). To reflect the refined Be occupancy on T3, the values of the T-site aver-

[1] Deposit item AM-10-013, CIF files. Deposit items are available two ways: For a paper copy contact the Business Office of the Mineralogical Society of America (see inside front cover of recent issue) for price information. For an electronic copy visit the MSA web site at http://www.minsocam.org, go to the *American Mineralogist* Contents, find the table of contents for the specific volume/issue wanted, and then click on the deposit link there.

TABLE 1. Chemical composition of nabesite (Petersen et al. 2002)

Mineral	Nabesite	
	wt%	apfu
SiO_2	62.4	4.06
BeO	6.26	0.98
CaO	0.13	0.01
Na_2O	13.8	1.74
K_2O	0.34	0.03
H_2O	18.05	3.92

TABLE 2. Bavenite composition based on 13 tetrahedral cations

	This study		Petersen et al. (1995)	
	wt%	apfu	wt%	apfu
SiO_2	59.2(3)	9.00(4)	58.5(3)	9.00(3)
Al_2O_3	5.4(2)	0.96(4)	5.60(8)	1.02(2)
CaO	23.6(2)	3.85(4)	24.2(2)	4.00(3)
ZnO	0.1(1)	0.02(1)		
Na_2O	0.1(1)	0.05(4)		
K_2O	0.01(1)	–		
BeO	8.335	3.04*	9.5(8)	3.5(3)
OH	3.000	3.04*	1.8(1)	1.8(1)
H_2O				0.92(5)
Total	99.75		99.60	
* Based on stoichiometry, and Be = OH = 4 – Al.				

TABLE 3. Overview of the results of the refinements for the three beryllium minerals

Mineral	Chemical formula*, Z, and space group	Unit cell of the single crystal	Unit cell from joint refinement	Joint refinement fit parameters
Bavenite	$Ca_4[Be_3AlSi_9O_{25}(OH)_3]$ $Z = 4$ $Cmcm$ (no. 63)	$a = 23.1965(7)$ Å $b = 4.9741(2)$ Å $c = 19.4221(6)$ Å $V = 2241.0(2)$ Å^3	$a = 23.159(2)$ Å $b = 4.9671(3)$ Å $c = 19.392(2)$ Å $V = 2230.6(4)$ Å^3	$R_p = 0.0197$ $wR_p = 0.0251$ $RF^2 = 0.08562$ $GooF = 1.45$ $R_{SXC} = 0.0575$
Leifite/IMA 2007-017	$Na_{6.2}K_{0.46}[Be_2Al_{2.66}Si_{15.34}O_{39}F_2]$ $Z = 1$ $P\bar{3}m$ (no. 164)	$a = 14.3446(8)$ Å $c = 4.8455(2)$ Å $V = 863.47(8)$ Å^3	$a = 14.3204(5)$ Å $c = 4.8376(2)$ Å $V = 859.16(7)$ Å^3	$R_p = 0.0071$ $wR_p = 0.0097$ $RF^2 = 0.0834$ $GooF = 3.21$ $R_{SXC} = 0.0980$
Nabesite	$Na_2[BeSi_4O_{10}]\cdot3.77\ H_2O$ $Z = 4$ $P2_12_12_1$ (no. 19)	$a = 9.7128(2)$ Å $b = 10.1352(2)$ Å $c = 11.8919(2)$ Å $V = 1170.65(3)$ Å^3	$a = 9.7175(5)$ Å $b = 10.1361(5)$ Å $c = 11.8878(7)$ Å $V = 1170.9(2)$ Å^3	$R_p = 0.0068$ $wR_p = 0.0086$ $RF^2 = 0.18170$ $GooF = 1.92$ $R_{SXC} = 0.0228$

* Formulae given are idealized except where non-T atom cation compositional variations occur, for which chemical analysis data are given.

age T-O bond lengths and the EPMA measured composition, T3 was assigned and fixed as 0.5 Be, 0.25 Si, and 0.25 Al and T4 as 0.75 Si and 0.25 Al giving an overall crystallographic unit-cell framework of the composition $[Be_{3.0}Al_{1.0}Si_{9.0}O_{28}]$, which fits well to the empirical data of $[Be_{3.04}Al_{0.96}Si_9O_{24.86}(OH)_{3.04}]$.

TABLE 4a. Positional coordinates (e.s.d. values in parentheses) resulting from the joint refinement of the single-crystal X-ray and the NPD data of bavenite

Atom	Wyck.	x	y	z	Occ.	U_{iso}
Ca1	16h	0.08223(2)	0.25504(7)	0.15368(2)	1	0.01166
Si1 (T1)	4c	0	0.7747(2)	¼	1	0.0091
Be1 (T2)	8g	0.1243(2)	0.8228(6)	¼	1	0.01079
Be_Si2/ Al_Si2/ Si_Si2 (T3)	8f	0	0.7213(3)	0.10447(5)	0.5 0.25 0.25	0.00593
Si_Al1/ Al_Al1 (T4)	8e	0.09395(3)	½	0	0.75 0.25	0.01079
Si3 (T5)	8e	0.17045(3)	0	0	1	0.00943
Si4 (T6)	16h	0.21395(2)	0.8627(1)	0.14410(3)	1	0.0084
O1	8f	0	0.5747(4)	0.18217(7)	1	0.00885
O2	8f	0	0.0360(4)	0.10927(8)	1	0.01115
O3	16h	0.05783(5)	0.5960(3)	0.06927(5)	1	0.01223
O4	16h	0.13132(5)	0.2378(3)	0.03387(6)	1	0.01215
O5	16h	0.20858(4)	0.8728(3)	0.06086(6)	1	0.01121
O6	16h	0.23302(5)	0.5612(3)	0.16604(5)	1	0.01084
O7	16h	0.15420(5)	0.9410(3)	0.18013(5)	1	0.01063
O8	8g	0.12101(6)	0.4963(4)	¼	1	0.0099
O9	8g	0.05790(6)	0.9578(4)	¼	1	0.00924
H1	8g	0.3413(6)	0.938(3)	¼	1	0.019(4)
H2	8f	0	0.099(6)	0.069(2)	0.5	0.028(8)

Notes: U_{iso} is given in Å^2. In the atom names x_y, the y indicates the atom site names according to Cannillo et al. (1966).

After refining all of the non-H atom positions and their anisotropic displacement parameters, the position of the first H atom H1 could be determined from a neutron Fourier difference map calculation as a peak with negative intensity. The position of H1 refined to $x = 0.3413(6)$, $y = 0.938(3)$, and $z = ¼$, which is significantly different from the position $x = 0.1$, $y = 0.267$, and $z = ¼$ proposed in the literature (Cannillo et al. 1966). The atomic displacement parameter of H was refined to $U_{iso} = 0.019(4)$ Å^2 (Tables 4a and 4b). H1 is attached to O8, a terminal O atom of the BeO$_4$ (T2) tetrahedra, with a bond distance of 0.92(2) Å. The H atom occupies a site that projects into an empty cavity of the structure and shows two weak hydrogen bonds to two crystallographically equivalent O atoms (O6) of the framework (Fig. 1). After the refinement of the structure including the first H, a new Fourier map was calculated and the second H position could also be found as a peak with negative intensity. The position of H2 refined to $x = 0$, $y = 0.099(6)$, and $z = 0.069(2)$. The occupancy of the H2 site was fixed to 0.5, a value derived from the occupancy of Be within the (Be/Al/Si)O$_4$ tetrahedra to which H2 is attached; this produces an overall crystallographic stoichiometry identical to that of the idealized bavenite, $Ca_4Be_3AlSi_9O_{25}(OH)_3$. The atomic displacement parameter of H2 refined to the very reasonable value $U_{iso} = 0.028(8)$ Å^2 (Tables 4a and 4b). H2 is attached to O2, a terminal O atom of the (Be/Al/Si)O$_4$ (T3) tetrahedra, with a bond distance of 0.85(4) Å (Fig. 1). The final profile fit achieved to the NPD data are shown in Figure 2. Our new structure model shows clear and significant improvements on that presented by Cannillo et al. (1966) defining the correct

TABLE 4b. Anisotropic atomic displacement factors (in Å^2, e.s.d. values in parentheses) resulting from the joint refinement of the single-crystal X-ray and the NPD data of bavenite

Atom	U_{11}	U_{12}	U_{13}	U_{22}	U_{23}	U_{33}
Ca1	0.0130(3)	−0.0029(2)	−0.0004(2)	0.0167(3)	0.0007(2)	0.0053(3)
Si1 (T1)	0.0079(4)	0	0	0.0123(5)	0	0.0071(4)
Be1 (T2)	0.009(2)	0.001(2)	0	0.017(2)	0	0.007(2)
Be_Si2/Al_Si2/Si_Si2 (T3)	0.0053(5)	0	0	0.0102(6)	0.0003(4)	0.0023(4)
Si_Al1/Al_Al1 (T4)	0.0133(4)	0	0	0.0137(4)	0.0000(4)	0.0054(4)
Si3 (T5)	0.0092(4)	0	0	0.0146(4)	−0.0014(3)	0.0045(4)
Si4 (T6)	0.0092(3)	−0.0002(2)	0.0003(2)	0.0123(3)	0.0002(2)	0.0037(3)
O1	0.0079(7)	0	0	0.0134(9)	−0.0010(6)	0.0052(7)
O2	0.0110(8)	0	0	0.0139(9)	0.0015(6)	0.0085(7)
O3	0.0120(6)	0.0016(5)	0.0030(5)	0.0162(7)	−0.0007(5)	0.0085(5)
O4	0.0132(6)	0.0016(5)	0.0008(5)	0.0163(7)	−0.0034(4)	0.0070(5)
O5	0.0123(6)	0.0000(5)	−0.0002(5)	0.0163(7)	0.0004(5)	0.0051(5)
O6	0.0117(6)	−0.0001(5)	0.0022(5)	0.0130(6)	0.0010(5)	0.0079(5)
O7	0.0124(6)	0.0013(5)	0.0026(5)	0.0136(7)	0.0019(5)	0.0058(5)
O8	0.0094(8)	0.0000(6)	0	0.013(1)	0	0.0077(7)
O9	0.0095(7)	0.0004(6)	0	0.0141(9)	0	0.0041(7)

Notes: In the atom names x_y, the y indicates the atom site names according to Cannillo et al. (1966).

TABLE 5. Comparison of the bond lengths within the TO_4 tetrahedra with T = Be, Si, Al, Be/Al from our new structure model for bavenite with the model from Cannillo et al. (1966)

		Our model		Cannillo et al.	
T1	Si1-O9 (2×)	1.620(2)	Si1-O9 (2×)	1.604(5)	
	Si1-O1 (2×)	1.648(2)	Si1-O1 (2×)	1.650(5)	
T2	Be1-O8 (1×)	1.624(3)	Be1-O8 (1×)	1.68(2)	
	Be1-O7 (2×)	1.631(2)	Be1-O7 (2×)	1.606(7)	
	Be1-O9 (1×)	1.676(3)	Be1-O9 (1×)	1.67(2)	
T3	Be/Al/Si_Si2-O2 (1×)	1.566(2)	Si2-O2 (1×)	1.549(6)	
	Be/Al/Si_Si2-O3 (2×)	1.627(1)	Si2-O3 (2×)	1.600(5)	
	Be/Al/Si_Si2-O1 (1×)	1.674(2)	Si2-O1 (1×)	1.685(5)	
T4	Si/Al_Al1-O3 (2×)	1.653(1)	Al1-O3 (2×)	1.726(5)	
	Si/Al_Al1-O4 (2×)	1.696(1)	Al1-O4 (2×)	1.732(6)	
T5	Si3-O5 (2×)	1.604(1)	Si3-O5 (2×)	1.605(5)	
	Si3-O4 (2×)	1.627(1)	Si3-O4 (2×)	1.622(6)	
T6	Si4-O7 (1×)	1.598(1)	Si4-O7 (1×)	1.594(5)	
	Si4-O6 (1×)	1.618(1)	Si4-O6 (1×)	1.608(7)	
	Si4-O5 (1×)	1.620(1)	Si4-O5 (1×)	1.616(5)	
	Si4-O6 (1×)	1.631(1)	Si4-O6 (1×)	1.638(6)	

Notes: The values given in angstroms; e.s.d. values in parentheses.

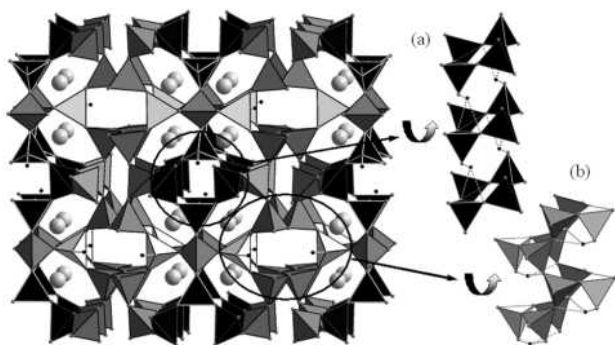**FIGURE 1.** Overview (along *b*) and details of the structure of bavenite. (**a**) shows the environment of H2 with two weak hydrogen bonds to O3. (**b**) shows the environment of H1 forming two weak hydrogen bonds to O6. Be (T2) atoms within the very light gray tetrahedra, Si (T1, T5, T6) atoms within the medium gray tetrahedra, mixed Si/Al (T4) site within the dark gray tetrahedra, mixed Be/Al/Si (T3) site within the black tetrahedra with white borders, O atoms: small gray spheres, H atoms: small black spheres. H-bonds are drawn as dashed lines.

fully occupied H position, a second partially occupied OH unit, and the likely natures of the T3 and T4 sites. However, full definition of the disorder associated with the tetrahedral sites, especially T3, and improved location and occupancy parameters for H2 will require further information, for example high-quality single-crystal neutron diffraction data, should crystals of sufficient size become available.

For leifite/IMA 2007-017, it was difficult to obtain high-quality single-crystal X-ray data as the crystals were generally very small (20 × 20 × 60 μm) or twinned by intergrowth. However, a joint SXD-NPD refinement was undertaken and the structure model of the framework from Sokolova et al. (2002) was confirmed. Table 6 compares the chemical data (EPMA) of this study with data from the literature (references given in Table 6). The chemical analysis data are in agreement with most published data for leifite from other localities, but, as the table shows, the Al content can vary significantly between samples. The formula based on 41 anions is $Na_6(K_{0.46}Na_{0.30}Cs_{0.01})_{\Sigma0.77}$ $(Si_{15.7}Al_{2.1}Be_2)_{\Sigma19.8}O_{38.95}F_{2.05}$. Table 6 confirms the presence of

F, and the improvement in the atomic displacement parameter with occupancy by F compared to O, together with improved bond lengths arguments, showed the presence of BeO_3F with F positioned on $x = ^1/_3$, $y = ^2/_3$, and $z = 0.0397(8)$. Aluminum was allocated to a mixed Si1/Al1 site with a fixed ratio to charge balance the analytical formula. The larger cations in leifite/ IMA 2007-017, Na, K and Cs, are distributed within the two differently shaped channel types of the structure. Within these channels there are three crystallographic sites that are either fully or partially occupied (Fig. 3). In the channels with a lenticular cross-section, the site Na1 was assumed to be fully occupied with Na ions by Sokolova et al. (2002); this is substantiated by our refinements. In the other channel with a near circular cross-section are two crystallographic sites proposed by Sokolova et al. (2002), denoted A and B, containing Na2 (0 0 0) and O6 (0 0 ½), respectively; O6 was assumed to be partially occupied with water (63%) and Na2 represented a mixed site for Na and further cations if present. O6 is positioned between two Na2 atoms at 2.418(1) and 2.547(1) Å from other framework O atoms. Our refinements performed with that model resulted in a very low occupancy for O6 of 17(2)% with a comparatively small atomic displacement parameter of 0.002(12) $Å^2$. The same has been found in IMA 2007-017 (Larsen et al. in prep). The site "Na2" is 3.128(3) Å from the framework O atoms, a distance more consistent with the larger K$^+$ ions than for Na ions. In conclusion, we assumed, due to bond distance reasons, that the site 0 0 ½ ("O6") is likely to be occupied by Na and the site 0 0 0 ("Na2") by K. This model (Table 7a) refined well and in fact significantly better than the model proposed previously by Sokolova et al. (2002). The occupancies of the cations were fixed following the EPMA analysis performed (Table 6) to 20% of Na on (0 0 ½) and 46% of K on (0 0 0) indicating a cation disorder in that channel, with only one of Na or K present on adjacent sites. The detected Cs was not considered, due to its very low fraction of 0.01 atoms per formula unit. The anisotropic atomic displacement parameters of the Na site were refined and resulted in an elongated ellipsoid (Table 7b) indicating a low level of local disorder of this ion along the channel axis. The new model (Fig. 3) does not need the presence of any water in
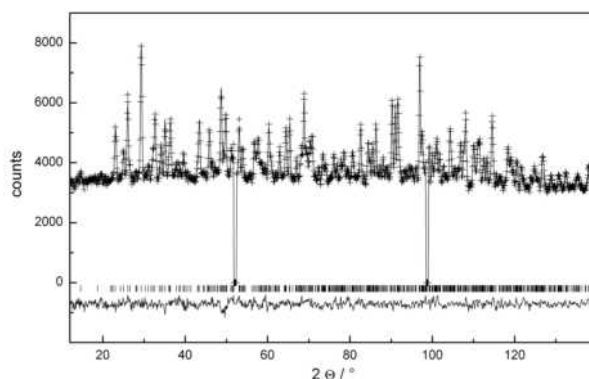

FIGURE 2. Plot of the fit for the NPD pattern from the joint refinement of single-crystal X-ray and NPD of bavenite $Ca_4[Be_{2.91(1)}$ $Al_{1.09(1)}Si_9O_{25}(OH)_{2.91}]$. Two small regions had to be excluded due to peaks resulting from the cryostat of the D20 diffractometer.

TABLE 6. Comparison of leifite composition from this study and the literature

Locality	NAR*		NAR†		ILI‡		MSH§		MSH§		MSH§		Kola§		VES‖	
	wt%	apfu	wt%	apfu	wt%	apfu	wt%	apfu	wt%	apfu	wt%	apfu	wt%	apfu	wt%	apfu
SiO$_2$	68.8(7)	15.7(2)	72.6	16.13	67.06	15.01	68.86	15.74	69.96	15.66	68.32	15.34	69.65	15.67	63.49	14.61
Al$_2$O$_3$	7.7(7)	2.1(1)	9.6	2.52	10.98	2.90	7.29	1.96	8.50	2.24	9.69	2.56	8.05	2.13	11.22	3.04
B$_2$O$_3$			0.5	0.19												
ZnO							1.02	0.17	0.09	0.02	0.37	0.06	0.71	0.12		
BeO	3.65	2	3.8	2.03	3.89	1.45	3.64	2	3.72	2	3.71	2	3.71	2	3.75	2.07
Na$_2$O	14.2	6.3(1)	12.4	5.34	13.94	6.05	14.82	6.57	14.75	6.39	14.17	6.17	14.78	6.44	13.77	6.14
K$_2$O	1.5(2)	0.46(6)			2.19	0.62	0.35	0.10	0.51	0.15	2.00	0.57	0.71	0.20	3.12	0.92
Cs$_2$O	0.07(4)	0.01(1)			0.77	0.07	0.48	0.05	0.09	0.01	0.01	–	0.04	–	0.39	0.04
Rb$_2$O							0.72	0.11	0.42	0.06	0.51	0.07	0.31	0.05	0.81	0.12
MgO															0.09	0.03
CaO															0.02	0.01
F	2.83(9)	2.05(6)	0.8	0.56	2.04	1.45	2.34	1.69	2.93	2.07	2.86	2.03	2.99	2.12	2.8	2.04
H$_3$O$_2$			2.7#	2.83												
OH			0.3#	0.44											0.63	0.97

Notes: Locality key: NAR, Narssârssuk Pegmatite; ILI, Ilímaussaq Alkaline Complex; MSH, Mont Saint-Hilaire; Kola, Kola Peninsula; VES, Vesle Arøya, Langesundsfjord.
* This study; average of 21 analyses.
† Micheelsen and Petersen (1970).
‡ Petersen et al. (1994).
§ Sokolova et al. (2002).
‖ Larsen and Åsheim (1995).
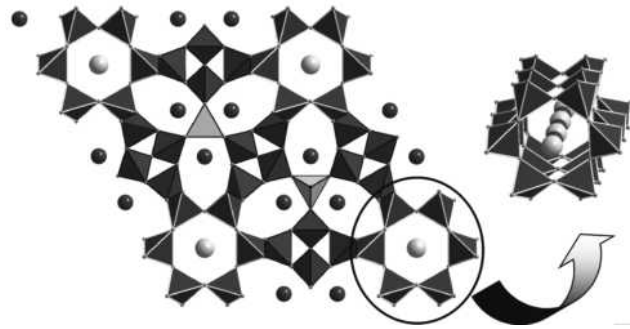\# In the paper, the wt% oxides are given as H$_2$O.

FIGURE 3. Overview (left, view along *c*) of the structure of leifite/IMA 2007-017. Channel with disordered Na (about 20%) and K (about 46%) atoms. Note that not all of the cations are present at a time. Beryllium atoms within the very light gray tetrahedra, Si atoms within the dark gray tetrahedra, mixed Al/Si site within the dark gray tetrahedra with white borders; O atoms are represented by small gray spheres, and F atoms by small black spheres.

the structure, which is also consistent with TGA measurements that we performed and the fact that it was impossible to find any H positions connected to the formerly proposed O site O6 (now Na). The resulting formula from this work is therefore Na$_{6.2}$K$_{0.46}$[Be$_2$Al$_{2.66}$Si$_{15.34}$O$_{39}$F$_2$]. Based on our structural and chemical data, the analyzed material indicates a solid solution between leifite and the Na end-member, where this material is closer to the IMA 2007-017 than the leifite end-member.

Nabesite, with four water molecules, has eight different crystallographic sites for hydrogen and presented an excellent, but challenging structure refinement using the combined NPD-SXD method. A full final, stable refinement (Table 3) with anisotropic atomic displacement parameters for all non-H atoms and isotropic ones for the H atoms (Tables 8a and 8b) was achieved. For the refinement of the H atom positions, soft constraints, restricting the distance of the H atom to the O of the water molecule to 0.940(1) Å, were applied. The structure of the framework described in the literature (Petersen et al. 2002) was confirmed, as well as the positions of the H atoms for three of the

four water molecules (H$_2$Ow1, H$_2$Ow2, and H$_2$Ow4). The fourth water molecule H$_2$Ow3 adopts a different position from the one previously proposed with dissimilar refined coordinates for the H atoms H5 and H6 (Table 8a). These two H atoms are involved in two weak hydrogen bonds. H6 forms a hydrogen bond with the O atom of the H$_2$Ow4 water molecule, and H5 forms a hydrogen bond with the framework O atom O2 (Fig. 4).

We have also analyzed NPD data in combination with SXD

TABLE 7a. Positional coordinates (e.s.d. values in parentheses) resulting from the joint refinement of the single-crystal X-ray and the NPD data of leifite/IMA 2007-017 Na$_{6.2}$K$_{0.46}$[Be$_2$Al$_{2.66}$Si$_{15.34}$O$_{39}$F$_2$]

Atom	Wyck.	*x*	*y*	*z*	Occ.	U_{iso}
Na1	6*i*	0.7508(1)	0.2492(1)	0.2019(4)	1	0.01395
K1(Na2)	1*a*	0	0	0	0.4600	0.00953
Na2(O6)	1*b*	0	0	½	0.2000	0.030(8)
Si1A	6*h*	0	0.21634(14)	½	0.5567	0.01242
Al1B					0.4433	
Si2	6*g*	0	0.34374(12)	0	1	0.01243
Si3	6*i*	0.44746(7)	0.55254(7)	0.30616(28)	1	0.00777
Be1	2*d*	0.333300	0.666700	0.3685(8)	1	0.01543
O1	6*i*	0.10022(13)	0.89978(13)	0.3903(5)	1	0.02148
O2	12*j*	0.30901(15)	0.26112(16)	0.2495(4)	1	0.01413
O3	12*j*	0.35849(14)	0.45743(15)	0.1026(4)	1	0.00813
O4	3*f*	0.500000	0.000000	0.500000	1	0.01099
O5	6*i*	0.39389(10)	0.60612(10)	0.4835(5)	1	0.00718
F	2*d*	0.333300	0.666700	0.0397(8)	1	0.01015

Note: U_{iso} is given in Å^2.

TABLE 7b. Anisotropic atomic displacement factors (in Å^2, e.s.d. values in parentheses) resulting from the joint refinement of the single-crystal X-ray and the NPD data of leifite/IMA 2007-017 Na$_{6.2}$K$_{0.46}$[Be$_2$Al$_{2.66}$Si$_{15.34}$O$_{39}$F$_2$]

Atom	U_{11}	U_{12}	U_{13}	U_{22}	U_{23}	U_{33}
Na1	0.014(1)	0.006(2)	0.0009(4)	0.014(1)	–0.0009(4)	0.013(2)
K1(Na2)	0.013(3)	0.006(2)	0	0.013(3)	0	0.003(3)
Si1A/Al1B	0.009(1)	–0.0032(5)	–0.0015(7)	0.0058(8)	–0.0008(4)	0.0137(8)
Si2	0.011(1)	0.0056(5)	–0.0002(6)	0.0108(7)	–0.0001(4)	0.0154(8)
Si3	0.0083(7)	0.0051(8)	–0.0000(3)	0.0083(7)	0.0000(3)	0.0079(7)
Be1	0.020(2)	0.0100(9)	0	0.020(2)	0	0.006(3)
O1	0.018(2)	–0.004(2)	–0.0009(7)	0.018(2)	0.0009(7)	0.012(2)
O2	0.017(2)	0.0055(9)	0.0067(9)	0.008(2)	0.0044(9)	0.017(1)
O3	0.009(2)	0.009(1)	0.0010(8)	0.009(2)	–0.0016(8)	0.012(1)
O4	0.014(2)	0.007(2)	0.0024(8)	0.013(3)	0.005(2)	0.006(2)
O5	0.008(2)	0.005(2)	0.0022(5)	0.008(2)	–0.0022(5)	0.007(2)
F	0.012(2)	0.0057(8)	0	0.012(2)	0	0.008(3)

TABLE 8a. Positional coordinates (e.s.d. values in parentheses) resulting from the joint refinement of the single-crystal X-ray and the NPD data of nabesite Na$_2$[BeSi$_4$O$_{10}$]·3.77 H$_2$O

Atom	Wyck.	x	y	z	Occ.	U_{iso}
Na1	4a	0.02305(4)	0.19135(4)	0.81969(4)	1	0.0124
Na2	4a	0.36397(4)	0.25068(4)	0.74081(4)	1	0.01603
Be1	4a	0.2419(2)	0.2631(2)	0.25732(9)	1	0.00681
Si1	4a	0.07752(3)	0.35377(3)	0.06705(2)	1	0.00566
Si2	4a	0.40206(3)	0.36422(3)	0.44736(2)	1	0.00574
Si3	4a	0.28527(3)	0.14862(3)	0.03361(2)	1	0.00577
Si4	4a	0.20469(3)	0.14805(3)	0.48034(2)	1	0.00574
O1	4a	0.11450(7)	0.34306(6)	0.19655(5)	1	0.00713
O2	4a	0.11804(7)	0.49547(5)	0.01178(5)	1	0.00873
O3	4a	−0.08718(6)	0.33002(6)	0.05361(5)	1	0.00797
O4	4a	0.15832(7)	0.24267(6)	−0.00831(5)	1	0.00693
O5	4a	0.34677(7)	0.36601(6)	0.32177(5)	1	0.00707
O6	4a	0.56498(7)	0.32750(6)	0.44779(5)	1	0.00871
O7	4a	0.31877(6)	0.25543(6)	0.52376(5)	1	0.00667
O8	4a	0.32601(7)	0.18187(6)	0.15891(5)	1	0.00755
O9	4a	0.23591(7)	−0.00391(6)	0.01777(5)	1	0.00805
O10	4a	0.18103(7)	0.15696(6)	0.34853(5)	1	0.0084
Ow1	4a	0.21315(8)	0.07221(7)	0.76340(5)	0.931(3)	0.00648
Ow2	4a	0.15355(7)	0.37184(6)	0.74025(5)	0.953(3)	0.00968
Ow3	4a	−0.06814(8)	0.02190(7)	0.95231(6)	0.951(3)	0.013
Ow4	4a	0.47553(7)	0.43982(7)	0.80646(6)	0.931(3)	0.00976
H1	4a	0.250(2)	0.003(1)	0.807(1)	0.931(3)	0.055(4)
H2	4a	0.181(2)	0.030(2)	0.6983(8)	0.931(3)	0.076(6)
H3	4a	0.158(2)	0.4514(7)	0.781(1)	0.953(3)	0.055(4)
H4	4a	0.099(2)	0.384(2)	0.6757(9)	0.953(3)	0.092(6)
H5	4a	−0.1577(6)	0.021(2)	−0.018(2)	0.951(3)	0.079(6)
H6	4a	−0.015(2)	0.018(2)	1.018(1)	0.951(3)	0.116(7)
H7	4a	0.442(2)	0.5172(6)	0.7727(9)	0.931(3)	0.025(3)
H8	4a	0.5524(9)	0.426(2)	0.7601(9)	0.931(3)	0.051(4)

Notes: U_{iso} is given in Å^2.

TABLE 8b. Anisotropic atomic displacement factors (in Å^2, e.s.d. values in parentheses) resulting from the joint refinement of the single-crystal X-ray and the NPD data of nabesite Na$_2$[BeSi$_4$O$_{10}$]·3.77 H$_2$O

Atom	U_{11}	U_{12}	U_{13}	U_{22}	U_{23}	U_{33}
Na1	0.0102(2)	0.0019(2)	−0.0014(2)	0.0127(2)	−0.0038(2)	0.0144(2)
Na2	0.0176(3)	0.0005(2)	−0.0016(2)	0.0124(2)	0.0009(2)	0.0180(3)
Be1	0.0061(6)	0.0010(4)	−0.0018(5)	0.0074(6)	0.0005(4)	0.0070(6)
Si1	0.0055(2)	0.00038(9)	−0.0005(1)	0.0049(2)	0.0004(1)	0.0066(2)
Si2	0.0058(2)	−0.00062(9)	−0.00018(9)	0.0047(2)	−0.0004(1)	0.0067(2)
Si3	0.0056(2)	0.00025(9)	−0.0001(1)	0.0049(2)	−0.00018(9)	0.0067(2)
Si4	0.0057(2)	−0.00071(9)	−0.0002(1)	0.0048(2)	0.00014(9)	0.0067(2)
O1	0.0069(4)	0.0014(3)	−0.0012(3)	0.0066(4)	−0.0004(3)	0.0079(4)
O2	0.0110(4)	0.0001(3)	−0.0001(3)	0.0059(4)	0.0008(3)	0.0093(4)
O3	0.0071(4)	−0.0001(3)	0.0000(3)	0.0090(4)	0.0008(3)	0.0079(4)
O4	0.0080(4)	0.0003(3)	−0.0005(3)	0.0060(4)	−0.0002(3)	0.0068(4)
O5	0.0077(4)	−0.0009(3)	−0.0010(3)	0.0051(3)	0.0001(3)	0.0084(3)
O6	0.0072(4)	0.0002(3)	−0.0002(3)	0.0104(4)	−0.0018(3)	0.0086(4)
O7	0.0078(4)	0.0001(3)	−0.0001(3)	0.0055(4)	−0.0003(3)	0.0067(4)
O8	0.0071(4)	0.0012(3)	−0.0006(3)	0.0073(4)	−0.0000(3)	0.0082(4)
O9	0.0082(4)	−0.0005(3)	0.0011(3)	0.0067(4)	−0.0005(3)	0.0093(4)
O10	0.0090(4)	−0.0018(3)	−0.0014(3)	0.0077(4)	0.0003(3)	0.0085(4)
Ow1	0.0110(4)	0.0035(3)	−0.0027(3)	0.0039(4)	−0.0008(3)	0.0045(4)
Ow2	0.0149(4)	0.0006(3)	−0.0021(3)	0.0065(4)	−0.0016(3)	0.0077(4)
Ow3	0.0136(5)	−0.0032(3)	−0.0024(4)	0.0127(4)	0.0007(4)	0.0127(4)
Ow4	0.0109(4)	0.0025(3)	0.0002(4)	0.0074(4)	0.0059(3)	0.0110(4)

data for epididymite and eudidymite (from Kvanefjeld, Ilímaussaq alkaline complex, South Greenland, and Vesle Arøya, Langesundsfjord, Norway, respectively) and obtained results that are in excellent agreement with those obtained by Gatta et al. (2008) in a recent independent study of epididymite and eudidymite (from Malosa, Malawi) by single-crystal neutron diffraction. Similarly, for semenovite-(Ce) and sørensenite refinements performed using the NPD data alone confirmed the published structure models derived from SXD data by Mazzi et al. (1979) and by Metcalf-Johansen and Hazell (1976), respectively. In both these cases, hydrogen positions could be freely refined with our neutron data and precise O-H nuclear distances extracted.

Discussion of the combined SXD-NPD method applied to mineralogy

The combined SXD-NPD analysis method described above proved successful for several complex Be framework materials and can be usefully applied to many other natural mineral systems. In this paper, the technique has shown to provide new structural information for bavenite, nabesite, and leifite/IMA 2007-017. As single crystals of a size and quality suitable for SND are rarely available and that technique requires long experiment times, the joint SXD/NPD method offers a much more facile route to the structures of minerals containing H. Furthermore as the technique only requires small amounts, typically a few hundred milligrams, of polycrystalline material, small single crystals suitable for SXD, and short periods of neutron beam time (a few hours for NPD rather than several days for SND), it becomes far easier to collect structural data from several specimens, including those from different localities. Therefore, the effects of variations in specimen composition and locality on a crystal structure become amenable to study. Given the widespread occurrence of H in minerals, often in combination with high atomic number elements that dominate the scattering in X-ray diffraction studies, the method can rapidly provide information on the distribution of H where crystallographic models from SXD analysis alone is not definitive. We have previously studied several natural hydrated zeolites including those from the scolecite, mesolite, natrolite system, and published results of our analysis of gooscreekite (Henry et al. 2008). In these systems, accurate definition of the water molecule orientations become possible and many other hydrated minerals are amenable to study using this technique. Therefore significant improvements in the quality of structural data can be obtained for minerals containing light atoms, such as H and Be, by employing NPD data collected on medium-resolution high-flux instruments. Other mineral classes
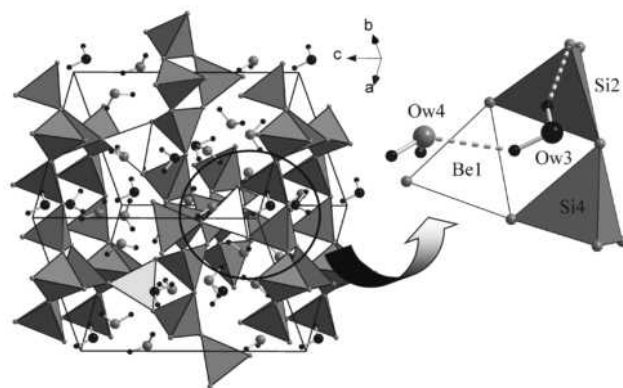

FIGURE 4. Overview and detail of the structure of nabesite. The two H atoms H6 (left) and H5 (right) of the water molecule H$_2$Ow3 are involved in two weak hydrogen bonds. H6 forms a hydrogen bond with the O atom of the H$_2$Ow4 water molecule and H5 forms a hydrogen bond with the framework O atom O2. Beryllium atoms within the very light gray tetrahedra, Si atoms within the medium gray tetrahedral; framework O atoms are represented by small gray spheres, and water O atoms by large gray spheres (Ow4) and large dark spheres (Ow3). Hydrogen bonds drawn as dashed lines.

and naturally occurring materials that could benefit enormously from application of this method include many clay minerals, hydrated salts and hydroxides, and clathrates.

REFERENCES CITED

Artini, E. (1901) Di una nuova specie minerale trovata nel granito di Baveno. Atti della Reale Accademia dei Lincei. Rendiconti. Classe di Scienze Fisiche, Matematiche e Naturali, 10, 139–145.

Baerlocher, Ch., Meier, W.M., and Olson, D.H. (2007) Atlas of Zeolite Framework Types. Elsevier, Amsterdam.

Beus, A.A. (1960) Geochemistry of Beryllium and Genetic Types of Beryllium Formations, p. 287. Izvestiya Akademii Nauk SSSR, Moscow (in Russian). Freeman, San Francisco, California.

Bøggild, O.B. (1915) Leifite, et nyt mineral fra Narsarsuk. Meddelelser Om Grønland, 51, 427–433.

Cannillo, E., Coda, A., and Fagnani, G. (1966) The crystal structure of bavenite. Acta Crystallographica, 20, 301–309.

Coda, A., Ungaretti, L., and Della Giusta, A. (1974) The crystal structure of leifite, $Na_6[Si_{16}Al_2(BeOH)_2O_{39}] \cdot 1.5H_2O$. Acta Crystallographica, B30, 396–401.

Gatta, G.D., Rotiroti, N., McIntyre, G.J., Guastoni, A., and Nestola, F. (2008) New insights into the crystal chemistry of epididymite and eudidymite from Malosa, Malawi: A single-crystal neutron diffraction study. American Mineralogist, 93, 1158–1165.

Hansen, T.C., Henry, P.F., Fischer, H.E., Torregrossa, J., and Convert, P. (2008) The D20 instrument at the ILL: A versatile high-intensity two-axis neutron diffractometer. Measurement Science and Technology, 19, 1–6.

Hawthorne, F.C. and Huminicki, D.M.C. (2002) The crystal chemistry of beryllium. In E.S. Grew, Ed., Beryllium: Mineralogy, Petrology, and Geochemistry, 50, p. 333–403. Reviews in Mineralogy and Geochemistry, Mineralogical Society of America, Chantilly, Virginia.

Henry, P.F., Weller, M.T., and Wilson, C.C. (2008) Hydogenous materials using powder neutron diffraction: full structural determination of adsorbed water molecules in a zeolite. Chemical Communications, 1557–1559.

Larsen, A.O. and Åsheim, A. (1995) Leifite from a nepheline syenite pegmatite on Vesle Arøya in the Langesundsfjord district, Oslo Region, Norway. Norsk Geologisk Tidsskrift, 75, 243–246.

Larson, A.C. and Von Dreele, R.B. (2004) General Structure Analysis System, GSAS. Los Alamos National Laboratory, New Mexico, Report LAUR 86-748.

Mazzi, F., Ungaretti, L., Dal Negro, A., Petersen, O.V., and Rønsbo, J.G. (1979) The crystal structure of semenovite. American Mineralogist, 64, 202–210.

Metcalf-Johansen, J. and Hazell, R.G. (1976) The crystal structure of sorensenite, $Na_4SnBe_2(Si_3O_9)_2 \cdot 2H_2O$. Acta Crystallographica, B32, 2553–2556.

Micheelsen, H.I. and Petersen, O.V. (1970) Leifite, revised and karpinskyite, discredited. Bulletin of the Geological Society of Denmark, 20, 134–151.

Petersen, O.V., Rønsbo, J.G., Leonardsen, E.S., Johnsen, O., Bollingberg, H., and Rosehansen, J. (1994) Leifite from the Ilimaussaq Alkaline Complex, South Greenland. Neues Jahrbuch für Mineralogie, Monatshefte, 83–90.

Petersen, O.V., Micheelsen, H.I., and Leonardsen, E.S. (1995) Bavenite, $Ca_4Be_3Al[Si_9O_{25}(OH)_3]$, from the Ilimaussaq Alkaline Complex, South Greenland. Neues Jahrbuch für Mineralogie, Monatshefte, 321–335.

Petersen, O.V., Giester, G., Brandstätter, F., and Niedermayr, G. (2002) Nabesite, $Na_2BeSi_4O_{10} \cdot 4H_2O$, a new mineral species from the Ilímaussaq alkaline complex, South Greenland. Canadian Mineralogist, 40, 173–181.

Petricek, V., Dusek, M., and Palatinus, L. (2006) Jana2006. The crystallographic computing system. Institute of Physics, Praha, Czech Republic.

Pouchou, J.L. and Pichoir, F. (1984) Quantitative microanalytic possibilities using a new formulation of matrix effects. Journal de Physique, 45, 17–20.

Raade, G. (2008) Beryllium in alkaline rocks and syenitic pegmatites. Norsk Bergverksmuseums Skriftserie, 37, 1–69.

Rodríguez-Carvajal, J. (2001) Recent Developments of the Program FULLPROF. Commission on Powder Diffraction (IUCr) Newsletter, 26, 12–19.

Schaller, W.T. and Fairchild, J.G. (1932) Bavenite, a beryllium mineral, pseudomorphs after beryl, from California. American Mineralogist, 17, 409–422.

Sheldrick, G.M. (2008) A short history of SHELX. Acta Crystallographica, A64, 112–122.

Sokolova, E., Huminicki, D.M.C., Hawthorne, F.C., Agakhanov, A.A., Pautov, L.A., and Grew, E.S. (2002) The crystal chemistry of telyushenkoite and leifite, A $Na_6[Be_2Al_3Si_{15}O_{39}F_2]$, A = Cs, Na. Canadian Mineralogist, 40, 183–192.

Toby, B.H. (2001) EXPGUI, a graphical interface for GSAS. Journal of Applied Crystallography, 34, 210–213.

Weller, M.T., Henry, P.F., and Light, M.E. (2007) Rapid structure determination of the hydrogen-containing compound $Cs_2C_2O_4 \cdot H_2O$ by joint single-crystal X-ray and powder neutron diffraction. Acta Crystallographica, B63, 426–432.